Reactions of Laser-Ablated Rhenium Atoms with Carbon Dioxide: Matrix Infrared Spectra and Density Functional Calculations on $OReCO$, O_2ReCO, $ORe(CO)_2$, $O_2Re(CO)_2$, $OReCO^-$, and $ORe(CO)_2^-$

Binyong Liang and Lester Andrews*

Department of Chemistry, University of Virginia, P.O. Box 400319, Charlottesville, Virginia 22904-4319

Received: August 16, 2001; In Final Form: October 23, 2001

Laser-ablated rhenium atoms react with CO_2 molecules upon co-condensation in excess argon at 7 K and neon at 4 K. Besides neutral products [$OReCO$, O_2ReCO, $ORe(CO)_2$, and $O_2Re(CO)_2$], anionic species [$OReCO^-$, $ORe(CO)_2^-$] are formed and identified through annealing, ultraviolet irradiation, isotopic substitution, and CCl_4 doping experiments. DFT calculations have been performed on all product species, and the very good overall agreement between the calculated and the observed vibrational frequencies supports the product identifications.

I. Introduction

Carbon dioxide, an abundant carbon source in the atmosphere, is regarded as one main cause of the so-called "greenhouse effect". The possibility of using CO_2 as an alternative starting material for the syntheses of fine chemicals presents an attractive challenge to scientists in various disciplines. One most promising and widely adopted method uses transition metal (TM) catalysts, and CO_2 fixation has become a very active subject of research in organometallic and catalytic surface chemistry.[1−4] The coordination of CO_2 to a metallic center is the key step in the CO_2 reduction, but the intermediate species formed during the reactions are still unknown for many processes. Using thermal TM atom evaporation, complexes with first-row metals Ti through Cu have been studied in solid CO_2 matrixes.[5] Recent studies of the reactions between laser-ablated TM atoms and CO_2 have revealed ionic products in addition to neutral molecules.[6−11] Theoretical studies on neutral[12−14] and cationic[15,16] complexes of CO_2 and first-row transition metals have been reported, and different bonding schemes have been proposed for early and late transition metals.

Although rhenium based complexes have been widely used to study CO_2 activation and reduction,[17−20] little is known about the product structure, as well as the key coordination steps in these reactions. Also, to our knowledge, no theoretical investigations of rhenium and CO_2 have been reported. We present here an experimental and theoretical study of reaction products between laser-ablated rhenium and CO_2. Density functional theory (DFT) calculations performed here not only serve as an aid for spectroscopic assignment, but additionally, reveal the complicated nature of rhenium compounds.

II. Experimental and Computational Methods

The experimental method for laser ablation and matrix isolation has been described in detail previously.[21−24] Briefly, the Nd:YAG laser fundamental (1064 nm, 10 Hz repetition rate with 10 ns pulse width, 3−5 mJ/pulse) was focused to ablate the rotating rhenium target (Goodfellow Metals). Laser-ablated rhenium was co-deposited with carbon dioxide (0.2%-2%) in excess neon or argon onto a 4 K (neon) or 7 K (argon) CsI cryogenic window at 2−4 mmol/h for 0.5−1.5 h. Carbon dioxide (Matheson), isotopic $^{13}C^{16}O_2$ (Cambridge Isotopic Laboratories), 85% ^{18}O enriched CO_2 (Spectra Gases) and selected mixtures were used in different experiments. Infrared spectra were recorded at 0.5 cm^{-1} resolution on a Nicolet 750 (Ne) or Nicolet 550 (Ar) spectrometer with 0.1 cm^{-1} accuracy using a mercury cadmium telluride (MCTB) detector down to 400 cm^{-1}. Matrix samples were annealed at different temperatures, and selected samples were subjected to irradiation using a medium-pressure mercury lamp ($\lambda > 240$ nm) with the globe removed and applying optical filters when needed.

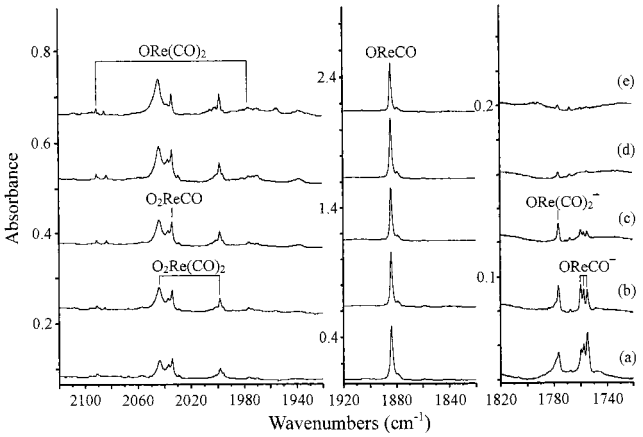

Figure 1. Infrared spectra in the 2120−1720 cm^{-1} region for laser-ablated Re co-deposited with 2% CO_2 in argon at 7 K. (a) sample deposited for 70 min, (b) after 30 K annealing, (c) after $\lambda > 290$ nm irradiation, (d) after $\lambda > 240$ nm irradiation, and (e) after 40 K annealing.

DFT calculations were performed on all of the proposed reaction products using the GAUSSIAN 98 program[25] and the B3LYP[26] functional. The 6-311+G* basis set was used for carbon and oxygen,[27] and the LanL2DZ effective core potential and basis for rhenium.[28] Such calculations were effective for identifying products in earlier TM-CO_2 reactions.[7−11]

III. Results

Infrared Spectra. *Re + CO_2 in Argon.* Figures 1 and 2 show the 2120−1720, 960−860 and 560−430 cm^{-1} regions of the

10.1021/jp013184s CCC: $22.00
Published on Web 01/04/2002

TABLE 1: Infrared Absorptions (cm^{-1}) from Reaction of Laser-Ablated Re Atoms with CO_2 in Excess Argon at 7 K

$^{12}C^{16}O_2$	$^{13}C^{16}O_2$	$^{12}C^{18}O_2$	12 + 13[a]	16 + 18[a]	R(12/13)	R(16/18)	assignment
2344.8	2279.2	2309.7			1.0288	1.0152	CO_2
2339.0	2273.6	2304.1			1.0288	1.0152	CO_2
2143.0	2095.8	2092.0			1.0225	1.0244	$(CO)_x$
2138.3	2091.1	2087.2			1.0226	1.0245	CO
2091.2	2042.8	2044.9	2072.6	2073.5	1.0237	1.0226	$ORe(CO)_2$
2085.1	2039.5	2035.0			1.0224	1.0246	?
2083.6	2037.5	2034.2			1.0226	1.0243	?
2044.0	1996.1	2000.4	2021.1	2023.5	1.0240	1.0218	$O_2Re(CO)_2$
2037.0	1983.3	2007.3			1.0271	1.0148	CO_3
2034.1	1987.1	1989.1			1.0237	1.0226	O_2ReCO
1998.3	1953.7	1952.0	1970.4	1969.8	1.0228	1.0237	$O_2Re(CO)_2$
1976.5	1930.7	1932.9	1942.4	1946.5	1.0237	1.0225	$ORe(CO)_2$
1883.9	1839.6	1844.1			1.0241	1.0216	OReCO
1858.7							?
1856.8	1806.5	1826.7			1.0275	1.0161	$C_2O_4^-$
1776.6	1734.7	1739.2	1751.7	1755.0	1.0242	1.0215	$ORe(CO)_2^-$
1759.8	1716.5	1725.2			1.0252	1.0201	$OReCO^-$
1757.6	1714.2	1723.2			1.0253	1.0200	$OReCO^-$ site
1754.8	1711.5	1720.7			1.0253	1.0198	$OReCO^-$ site
982.0	982.0	928.4		965.6		1.0577	O_2ReCO
969.8	969.8	919.0				1.0553	?
934.4	934.1	885.6				1.0551	OReCO
929.1	929.0	883.2		896.2		1.0520	O_2ReCO
923.3	923.1	874.9				1.0553	$OReCO^-$
918.8	918.4	869.0		909.5		1.0573	$O_2Re(CO)_2$
896.4	896.2	851.3		858.3		1.0530	$O_2Re(CO)_2$
663.5	644.6	653.5			1.0293	1.0153	CO_2
661.9	643.2	651.9			1.0291	1.0153	CO_2
537.0		519.3				1.0341	OReCO
452.4	444.8	442.2	448.2	445.7	1.0171	1.0231	$O_2Re(CO)_2$

[a] 12 + 13 equals to $^{12}C^{16}O_2 + {}^{13}C^{16}O_2$; 16 + 18 equals to $^{12}C^{16}O_2 + {}^{12}C^{16}O^{18}O + {}^{12}C^{18}O_2$. Only additional bands for metal-dependent species are listed.

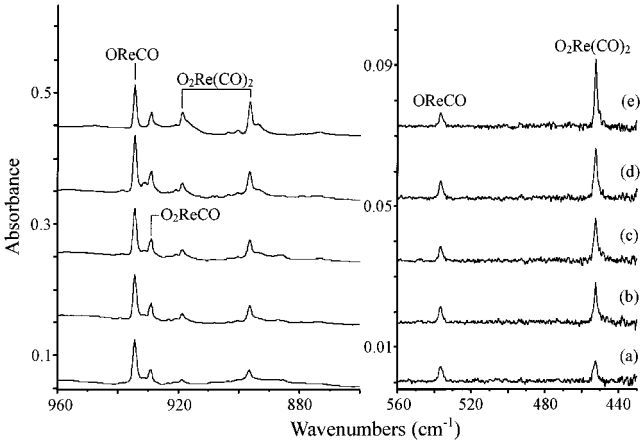

Figure 2. Infrared spectra in the 960−860 and 650−430 cm^{-1} regions for laser-ablated Re co-deposited with 2% CO_2 in argon at 7 K. (a) sample deposited for 70 min, (b) after 30 K annealing, (c) after $\lambda >$ 290 nm irradiation, (d) after $\lambda >$ 240 nm irradiation, (e) after 40 K annealing.

infrared spectra of reaction products of rhenium and 2% CO_2 in argon. The infrared absorptions are listed in the Table 1. Metal independent bands, including CO_3, $C_2O_4^-$, CO_2^-, have been reported elsewhere,[29−32] and will not be discussed in this paper. In the C−O stretching region, a very strong band was observed at 1883.9 cm^{-1} after deposition, and it almost did not change in the following annealing and ultraviolet irradiation operations. A new band at 2044.0 cm^{-1} also observed on deposition, increased on annealing and photolysis and is associated with the 1998.3 cm^{-1} absorption. Another band at 2034.1 cm^{-1} was sharper, and only showed significant increase on full-arc irradiation. Two other bands at 2091.2 and 1976.5 cm^{-1} tracked together throughout these experiments; both increased on annealing and irradiation. Two sets of bands were observed in the lower C−O stretching region: a triplet at 1759.8, 1757.6, and 1754.8 cm^{-1} was almost eliminated by $\lambda >$ 290 nm radiation, whereas the band at 1776.6 cm^{-1} only slightly decreased. Both bands did not recover on annealing following irradiation. In the Re−O stretching region, the strongest absorption at 934.4 cm^{-1} tracked with the 1883.9 cm^{-1} absorption in the C−O stretching region. The bands at 929.1 and 982.0 cm^{-1} tracked with the 2034.1 cm^{-1} band, and absorptions at 918.8, 896.4 cm^{-1} tracked with the 2044.0 cm^{-1} absorption. Two additional bands were observed below the CO_2 ν_2 absorption: a band at 537.0 cm^{-1} tracked with both 1883.9 and 934.4 cm^{-1} absorptions, whereas the 452.4 cm^{-1} band tracked with 2044.0, 1998.3, 918.8, and 896.4 cm^{-1} absorptions. The isotopic counterparts of all aforementioned bands are listed in the Table 1, and spectra from the mixed isotopic experiments are shown in Figures 3 and 4. Several bands showed triplet splitting patterns in the mixed isotopic experiments, and the additional bands are listed in the Table 1. For the mixed oxygen isotopic experiments, both $C^{16}O_2 + C^{18}O_2$ and $C^{16}O_2 + C^{16}O^{18}O + C^{18}O_2$ experiments were performed, and essentially the same spectra were produced.

Re + CO_2 in Neon. Figure 5 shows the 2120−1700 and 950−870 cm^{-1} infrared region of the reaction products between rhenium and 0.5% CO_2. The infrared absorptions are listed in Table 2. In the C−O stretching region, a new band sharpened to 1923.3 cm^{-1} on 12 K annealing, and a band at 1905.4 cm^{-1} separated into two sharp bands at 1905.4 and 1902.1 cm^{-1} after 12 K annealing. Several bands were observed near the 2044.9 cm^{-1} CO_3 absorption. On its red side, 2041.1 and 2038.3 cm^{-1} absorptions decreased after annealing and increased after irradiation. On its blue side, 2047.8 and 2051.1 cm^{-1} absorptions tracked with a band at 2003.3 cm^{-1} throughout the experiment. Two weak bands at 2092.8 and 1984.5 cm^{-1} were also observed

TABLE 2: Infrared Absorptions (cm^{-1}) from Reaction of Laser-Ablated Re Atoms with CO_2 in Excess Neon at 4 K

$^{12}C^{16}O_2$	$^{13}C^{16}O_2$	$^{12}C^{18}O_2$	12 + 13[a]	16 + 18[a]	R(12/13)	R(16/18)	assignment
2347.6	2281.8	2312.5			1.0288	1.0152	CO_2
2146.1	2098.8	2095.1			1.0225	1.0243	$(CO)_x$
2142.6	2095.4	2091.5			1.0225	1.0244	$(CO)_x$
2140.8	2093.7	2089.8			1.0225	1.0244	CO
2130.8	2074.5				1.0271		$C_2O_4^+$
2092.8	2046.5	2043.1	2074.6		1.0226	1.0243	$ORe(CO)_2$
2051.1	2003.6	2007.1	2028.3	2029.8	1.0237	1.0219	$O_2Re(CO)_2$ site
2047.8	2000.1	2003.7	2025.0	2026.9	1.0238	1.0220	$O_2Re(CO)_2$
2044.9	1991.1				1.0270		CO_3
2041.1	1993.9	1995.8			1.0237	1.0227	O_2ReCO
2038.3	1991.3	1993.2			1.0236	1.0226	O_2ReCO site
2003.3	1957.9	1957.1	1975.2	1966.8	1.0232	1.0236	$O_2Re(CO)_2$
1984.5	1941.1	1937.0	1956.9	1945.2	1.0224	1.0245	$ORe(CO)_2$
1923.3	1879.3	1881.3			1.0234	1.0223	OReCO
1905.4	1863.0	1861.9			1.0228	1.0234	OReCO site
1852.4	1802.9	1823.1			1.0275	1.0161	$C_2O_4^-$
1850.8	1801.0	1820.8			1.0277	1.0165	$C_2O_4^-$ site
1787.8	1745.0	1750.8	1760.2	1765.0	1.0245	1.0211	$ORe(CO)_2^-$
1771.1	1727.6	1736.2			1.0252	1.0201	$OReCO^-$
1670.1	1625.6	1642.3			1.0274	1.0169	$(CO_2)_2CO_2^-$
1665.3	1621.0	1637.6			1.0273	1.0169	$(CO_2)CO_2^-$
1658.2	1614.0	1630.5			1.0274	1.0170	CO_2^-
1421.6	1380.2	1399.6			1.0300	1.0157	CO_2^+
1274.4	1263.0	1227.5			1.0090	1.0382	$C_2O_4^+$
1256.4	1247.5				1.0071		CO_4^-
1189.2	1181.4				1.0066		$C_2O_4^-$
988.5	988.5	935.7		972.9		1.0564	O_2ReCO
940.0	940.0	893.5		906.5		1.0520	O_2ReCO site
938.5	938.9	892.0		904.9		1.0521	O_2ReCO
930.2	930.2	881.4				1.0554	$OReCO^-$
925.9	925.4	875.7		916.8		1.0573	$O_2Re(CO)_2$
913.6	913.2	865.7				1.0553	$ORe(CO)_2$
903.8	904.2	858.8		865.4		1.0524	$O_2Re(CO)_2$
668.2	649.1	658.3			1.0294	1.0150	CO_2

[a] 12 + 13 equals to $^{12}C^{16}O_2 + {}^{13}C^{16}O_2$; 16 + 18 equals to $^{12}C^{16}O_2 + {}^{12}C^{16}O^{18}O + {}^{12}C^{18}O_2$. Only additional bands for metal-dependent species are listed.

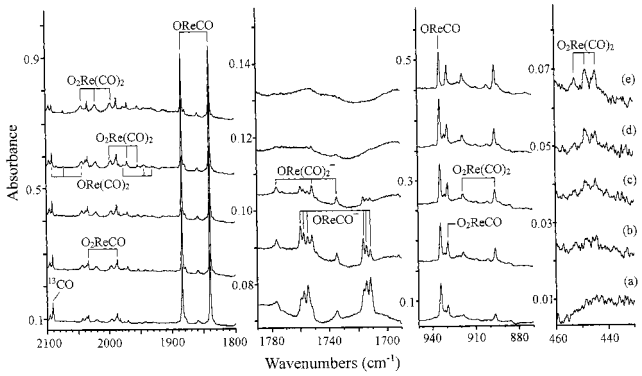

Figure 3. Infrared spectra in the 2100−1800, 1790−1690, 950−870, and 460−430 cm^{-1} regions for laser-ablated Re co-deposited with 0.7% $^{12}CO_2$ + 0.7% $^{13}CO_2$ in argon at 7 K. (a) sample deposited for 90 min, (b) after 30 K annealing, (c) after $\lambda > 290$ nm irradiation, (d) after $\lambda > 240$ nm irradiation, (e) after 40 K annealing.

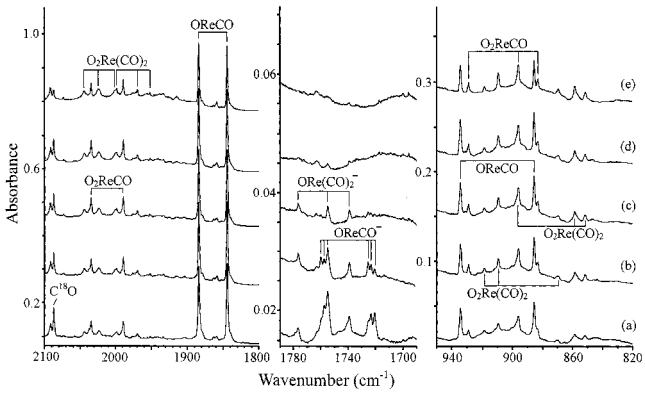

Figure 4. Infrared spectra in the 2100−1800, 1790−1690, and 950−820 cm^{-1} regions for laser-ablated Re co-deposited with 1% $C^{16}O_2$ + 1% $C^{18}O_2$ in argon at 7 K. (a) sample deposited for 90 min, (b) after 30 K annealing, (c) after $\lambda > 290$ nm irradiation, (d) after $\lambda > 240$ nm irradiation, (e) after 40 K annealing.

after deposition and increased markedly upon irradiation. Another strong band was observed at 1771.1 cm^{-1}, and in contrast to all aforementioned bands, this band was eliminated by mercury-arc irradiation. A weak photosensitive band was also observed at 1787.8 cm^{-1}. In the Re−O stretching region, a band at 938.5 cm^{-1} is associated with the 2041.1 cm^{-1} band. Two bands at 925.9 and 903.8 cm^{-1} tracked with 2047.8 and 2003.3 cm^{-1} bands. A weak photosensitive band was observed at 930.2 cm^{-1}. Figure 6 shows the spectra of laser-ablated rhenium with mixed $^{12}CO_2/^{13}CO_2$ samples; the corresponding isotopic absorptions are listed in the Table 2.

DFT Calculations. The ground state for Re atom was calculated as ^6S ($5d^56s^2$). The geometry for every proposed product molecule was optimized, and analytical second-derivatives were used to obtain the harmonic frequencies. For all molecules, calculations were done at different spin multiplicities. For converged spin states, we commonly switched occupied and virtual orbitals to confirm that the state under consideration was in fact the ground state. Different starting geometries were also used in the calculation: for the O_2ReCO example, the starting symmetry groups included C_{2v}, two different C_s, and C_1. The calculation results are summarized in the Tables 3 and 4. The ground states for all neutral molecules are doublets, and the anions are singlets except for $O_2Re(CO)_2^-$, which has a triplet ground state.

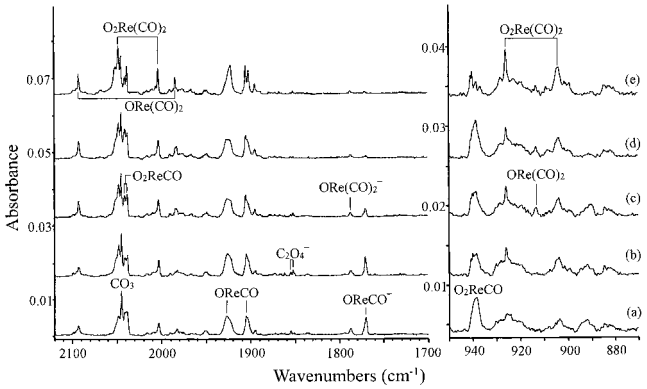

Figure 5. Infrared spectra in the 2120−1700 and 950−870 cm^{-1} regions for laser-ablated Re co-deposited with 0.2% CO_2 in neon at 4 K. (a) sample deposited for 30 min, (b) after 8 K annealing, (c) after $\lambda > 290$ nm irradiation, (d) after $\lambda > 240$ nm irradiation, and (e) after 12 K annealing.

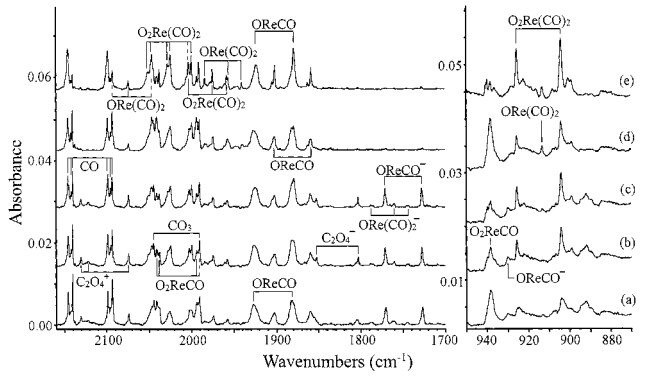

Figure 6. Infrared spectra in the 2160−1700 and 950−870 cm^{-1} regions for laser-ablated Re co-deposited with 0.15% $^{12}CO_2$ + 0.15% $^{13}CO_2$ in neon at 4 K. (a) sample deposited for 40 min, (b) after 8 K annealing, (c) after 10 K annealing, (d) after $\lambda > 240$ nm irradiation, and (e) after 12 K annealing.

IV. Discussion

OReCO. The bands at 1883.9, 934.4, and 537.0 cm^{-1} in the argon matrix are assigned to the OReCO molecule. The absorption at 1883.9 cm^{-1} red-shifted to 1839.6 and 1844.1 cm^{-1} in the $^{13}CO_2$ and $C^{18}O_2$ experiments, with carbon 12/13 and oxygen 16/18 isotopic frequency ratios of 1.0241 and 1.0216, respectively. In both $^{12}CO_2$ + $^{13}CO_2$ (Figure 3) and $C^{16}O_2$ + $C^{18}O_2$ (Figure 4) experiments, only doublets with two pure isotopic absorptions were observed. This absorption is appropriate for a C−O stretching mode, while the larger carbon 12/13 isotopic frequency ratio compared to the isolated CO molecule indicates that the carbon atom in the responsible molecule bonds to a heavy atom and exhibits M−C, C−O interaction. The associated mode at 934.4 cm^{-1} is appropriate for a Re−O vibration. This band showed very little carbon-13 isotopic shift but shifted to 885.6 cm^{-1} with $C^{18}O_2$ and gave an oxygen 16/18 isotopic frequency ratio of 1.0551, which is very close to the harmonic Re−O ratio of 1.0555. In the mixed $C^{16}O_2$ + $C^{16}O^{18}O$ + $C^{18}O_2$ experiment, only a doublet was observed. A third associated band at 537.0 cm^{-1} is very weak compared to other two bands. The band shifted to 519.3 cm^{-1} with $C^{18}O_2$, and showed a doublet in the mixed $C^{16}O_2$ + $C^{18}O_2$ experiment. Unfortunately, the $^{13}CO_2$ counterpart is too weak to be observed. This band is a predominantly Re−CO stretching mode according to the DFT displacement coordinates. Overall, these three bands at 1883.9, 934.4, and 537.0 cm^{-1}, with relative intensities 100:11:1, are assigned to the C−O, Re−O, and Re−CO stretching modes in the OReCO molecule, respectively.

Only one mode was observed in the neon matrix for this molecule. The band at 1923.3 cm^{-1} is assigned to the C−O stretching absorption of OReCO, displaced from the argon matrix value by 39.4 cm^{-1}. This band shifted to 1879.3 and 1881.3 cm^{-1} in $^{13}CO_2$ and $C^{18}O_2$ experiments, with isotopic ratios of 1.0234 and 1.0223, respectively. In both of the mixed isotopic experiments, only pure isotopic bands were observed. In addition, the 1905.4 cm^{-1} band is likely due to a matrix site of OReCO.

The ground state of OReCO was predicted as a planar $^2A'$ molecule with C_s symmetry. Other low-lying states included $^4A''$ and $^2A''$, only 2.5 and 10 kcal/mol higher in energy. The lowest sextet state is also converged as a linear molecule, at 11.4 kcal/mol higher in energy than the ground $^2A'$ state. The vibrational analyses for the ground $^2A'$ state predicted three modes at 1987.4, 974.4, and 552.1 cm^{-1} with relative intensities of 1390:204:26, which are in very good agreement with the argon matrix values. The argon matrix values require scale factors of 0.948, 0.959, 0.973 for three bands from higher to lower frequencies, respectively, which are typical for this functional.[33] For energy comparison, other isomers were calculated: $ReCO_2$ gave a C_{2v} symmetry, $^2A_2$ ground state 92 kcal/mol higher in energy than the ground-state OReCO molecule, and Re[OC]O (both C, O atoms bond to Re) yielded a C_s symmetry $^2A''$ ground state 51 kcal/mol higher.

$O_2Re(CO)_2$. In the argon matrix, the new band at 2044.0 cm^{-1} exhibited ^{13}C and ^{18}O counterparts at 1996.1 and 2000.4 cm^{-1}. This band split into triplets in both $^{12}CO_2$ + $^{13}CO_2$ and $C^{16}O_2$ + $C^{18}O_2$ experiments, with intermediate bands at 2021.1 and 2023.5 cm^{-1}, respectively. It is obvious that this is a C−O stretching mode of a dicarbonyl unit. Both intermediate bands blue-shifted by 1.1 and 1.3 cm^{-1}, respectively, from the medians of pure isotopic bands. The 1998.3 cm^{-1} absorption also revealed a triplet mixed isotopic spectrum with intermediate components at 1970.4 and 1969.8 cm^{-1}, red-shifted 5.6 and 5.4 from the medians of pure isotopic absorptions. Two associated absorptions at 918.8 and 896.4 cm^{-1} fall in the Re−O stretching region. Both bands showed very little change with $^{13}CO_2$ but shifted to 869.0 and 851.3 cm^{-1} in the $C^{18}O_2$ experiments, giving oxygen 16/18 isotopic frequency ratios of 1.0573 and 1.0530, respectively. The average of two isotopic ratios is 1.0552, very close to the same value in the ReO_2 molecule.[24] With mixed $C^{16}O_2$ + $C^{18}O_2$ (Figure 4), both bands showed skewed triplet features with the intermediate bands repelled greatly from the medians. The higher frequency intermediate band is 15.6 cm^{-1} higher, whereas the lower frequency intermediate band is 15.6 cm^{-1} lower than their respective medians. These two modes are appropriate for the symmetric and antisymmetric Re−O stretching modes in a ReO_2 unit. The fifth associated absorption at 452.4 cm^{-1} is appropriate for a Re−CO stretching mode. In the both mixed carbon-12/13 and oxygen-16/18 isotopic experiments, this band split into triplets, which once again confirmed that there are two CO subunits involved in the responsible molecule. We assign the bands at 2044.0, 1998.3, 918.8, 896.4, and 452.4 cm^{-1} to the symmetric C−O, antisymmetric C−O, symmetric ReO_2, antisymmetric ReO_2, and antisymmetric Re−CO stretching modes of $O_2Re(CO)_2$ in an argon matrix.

Four different modes were observed in the neon matrix for $O_2Re(CO)_2$. Two bands at 2047.8 and 2003.3 cm^{-1} tracked with each other throughout annealing and irradiation experiments, and both showed appropriate ^{13}C and ^{18}O isotopic shifts as carbonyl stretching modes. Each split into triplets in the mixed

TABLE 3: Equilibrium Geometry, and Frequencies Calculated for Products in the Reaction of Rhenium and CO_2[a]

species [b]		geometry (Å, degree)	frequencies (intensity)
OReCO	$^2A'$ (C_s) (0)	O−Re: 1.676, Re−C: 1.878, C−O: 1.158, ∠OReC: 105.4, ∠ReCO: 167.4	169.1(3), 395.2(32), 437.2(1), 552.1(26), 974.4(204), 1987.4(1390)
	$^4A''$ (C_s) (+2.5)	O−Re: 1.724, Re−C: 1.913, C−O: 1.154, ∠OReC: 110.8, ∠ReCO: 173.4	152.2(12), 414.5(0), 418.7(4), 509.9(14), 930.9(125), 2022.8(1022)
	$^2A''$ (C_s) (+10.0)	O−Re: 1.724, Re−C: 1.902, C−O: 1.156, ∠OReC: 109.0, ∠ReCO: 172.3	154.0(14), 421.0(2), 441.0(0), 520.2(19), 925.1(112), 2004.9(1178)
O_2ReCO	$^2A'$ (C_s) (0)	O−Re: 1.719, Re−C: 1.975, C−O: 1.141, ∠OReO: 132.2, ∠OReC: 113.1, ∠ReCO: 178.0	64.0(19), 124.1(1), 238.1(9), 404.2(10), 437.5(1), 482.4(5), 958.0(273), 1006.2(34), 2126.2(694)
	$^2A_1$ (C_{2v}) (+0.02)	O−Re: 1.720, Re−C: 1.975, C−O: 1.141, ∠OReO: 133.0	38.2i(27), 121.9(1), 241.0(7), 404.5(10), 432.6(0), 482.9(5), 957.2(280), 1003.9(37), 2127.8(668)
	$^4A''$ (C_s) (+29.7)	O−Re: 1.735, Re−C: 1.964, C−O: 1.149, ∠OReO: 115.2, ∠OReC: 111.7, ∠ReCO: 174.0	99.1(1), 125.6(14), 241.9(0), 270.8(10), 383.4(2), 482.1(5), 887.2(139), 939.4(136), 2036.3(986)
$ORe(CO)_2$	$^2A'$ (C_s) (0)	O−Re: 1.711, Re−C: 1.931, C−O: 1.151, ∠OReC: 113.7, ∠CReC: 100.8, ∠ReCO: 169.1	91.7(1), 144.9(10), 166.7(16), 416.1(1), 433.3(0), 457.9(2), 495.6(2), 496.8(48), 577.9(8), 962.6(122), 1995.4(1860), 2075.1(546)
	$^4B_1$ (C_{2v}) (+14.6)	O−Re: 1.729, Re−C: 1.980, C−O: 1.148, ∠OReC: 126.3, ∠ReCO: 172.9	75.7(0), 94.2(19), 122.3(4), 346.1(0), 375.4(0), 432.5(1), 472.5(39), 480.9(13), 522.0(16), 936.0(151), 2006.0(1901), 2076.6(363)
	$^2A_1$ (C_{2v}) (+14.7)	O−Re: 1.716, Re−C: 1.977, C−O: 1.150, ∠OReC: 127.7, ∠ReCO: 166.4	325.7i(20), 73.7(0), 81.4(41), 244.4(2), 378.9(5), 384.2(0), 435.4(3), 482.1(42), 563.0(21), 936.9(111), 1999.4(2108), 2081.0(262)
$O_2Re(CO)_2$	$^2A_2$ (C_{2v}) (0)	O−Re: 1.745, Re−C: 1.968, C−O: 1.142, ∠OReO: 116.2, ∠CReC: 99.0, ∠ReCO: 173.9, ∠OReC: 110.1	89.1(4), 94.8(0), 132.9(0), 140.2(76), 237.5(0), 255.7(9), 386.5(0), 406.6(51), 469.9(84), 474.1(0), 577.3(20), 856.7(204), 937.3(61), 1973.1(3511), 2139.5(419)
	$^2B_1$ (C_{2v}) (+1.5)	O−Re: 1.734, Re−C: 1.962, C−O: 1.147, ∠OReO: 123.9, ∠CReC: 81.8, ∠ReCO: 178.0, ∠OReC: 110.8	53.9(0), 64.2(85), 100.4(0), 124.3(0), 212.2(0), 252.4(4), 345.1(12), 426.9(43), 477.3(60), 504.7(0), 579.7(9), 939.1(180), 953.3(81), 1883.7(3719), 2123.8(460)
$OReCO^-$	$^1A'$ (C_s) (0)	O−Re: 1.717, Re−C: 1.831, C−O: 1.194, ∠OReC: 109.4, ∠ReCO: 166.1	181.3(6), 467.7(0), 530.4(2), 599.8(9), 944.3(155), 1827.7(1523)
	$^3A''$ (C_s) (+8.6)	O−Re: 1.763, Re−C: 1.871, C−O: 1.191, ∠OReC: 117.9, ∠ReCO: 169.2	159.2(12), 442.6(0), 479.2(9), 550.3(15), 859.8(205), 1801.7(2274)
$ORe(CO)_2^-$	$^1A'$ (C_s) (0)	O−Re: 1.763, Re−C: 1.891, C−O: 1.180, ∠OReC: 117.1, ∠CReC: 90.3, ∠ReCO: 168.7	95.5(1), 151.1(8), 158.7(14), 444.0(0), 468.9(0), 518.9(4), 540.8(6), 549.1(12), 624.3(4), 877.8(166), 1846.2(2065), 1920.2(1134)
	$^3A'$ (C_s) (+5.1)	O−Re: 1.773, Re−C: 1.921, C−O: 1.177, ∠OReC: 128.9, ∠CReC: 96.9, ∠ReCO: 169.9	67.7(7), 87.4(1), 119.1(19), 416.3(0), 440.2(0), 449.8(10), 502.3(3), 531.9(12), 615.4(12), 853.2(262), 1842.0(2274), 1925.5(539)
	$^1A_1$ (C_{2v}) (+19.6)	O−Re: 1.748, Re−C: 1.948, C−O: 1.171, ∠OReC: 126.1, ∠ReCO: 166.2	440.5i(622), 86.1(0), 106.4(35), 236.3(10), 377.6(10), 401.3(0), 456.9(11), 503.1(30), 599.2(8), 913.7(178), 1855.9(2900), 1962.6(275)
$O_2Re(CO)_2^-$	$^3B_2$ (C_{2v}) (0)	O−Re: 1.781, Re−C: 1.919, C−O: 1.175, ∠OReO: 115.1, ∠CReC: 89.4, ∠ReCO: 176.2, ∠OReC: 112.4	97.2(0), 107.1(4), 129.4(0), 169.4(6), 234.3(0), 252.1(0), 263.3(7), 466.6(6), 525.8(10), 530.3(0), 607.6(7), 814.6(250), 851.7(161), 1896.0(1476), 1964.0(646)
	^1A (C_2) (+7.0)	O−Re: 1.770, Re−C: 1.945, C−O: 1.173, ∠OReO: 120.9, ∠CReC: 73.1, ∠ReCO: 168.8, ∠OReC(1): 102.3, ∠OReC(2): 125.3	102.8(4), 105.6(0), 118.7(17), 149.0(5), 275.9(2), 357.9(3), 389.0(2), 484.9(1), 500.9(4), 515.2(4), 569.6(0), 870.2(256), 885.8(164), 1851.6(1634), 1965.3(794)

[a] DFT calculation: B3LYP funational, 6-311+G* basis set on C and O, LANL2DZ basis set and ECP on Re. [b] Two or three electronic states are listed for each species, labels in the first parentheses denote point groups, and numbers in the second parentheses denote the relative energies (kcal/mol) compared to the ground states.

carbon-12/13 or mixed oxygen-16/18 isotopic experiment. These two bands are the symmetric and anti-symmetric CO stretching modes, respectively, of the $O_2Re(CO)_2$ molecule. The symmetric and antisymmetric ReO_2 stretching modes were observed at

TABLE 4: Calculated Isotopic Frequencies for the Modes Observed in the Matrix Infrared Experiment

species	mode	$^{12}C^{16}O_2$	$^{13}C^{16}O_2$	$^{12}C^{18}O_2$	R(12/13)	R(16/18)
OReCO	a′	1987.4	1940.4	1943.5	1.0242	1.0226
	a′	974.4	974.4	923.1	1.0000	1.0556
	a′	552.1	542.5	537.5	1.0177	1.0272
O_2ReCO	a′	2126.2	2076.2	2078.8	1.0241	1.0228
	a′	1006.2	1006.2	950.6	1.0000	1.0585
	a″	958.0	958.0	910.3	1.0000	1.0524
$ORe(CO)_2$	a′	2075.1	2025.9	2029.7	1.0243	1.0224
	a″	1995.4	1949.6	1949.5	1.0235	1.0235
	a′	962.6	962.4	911.7	1.0002	1.0558
$O_2Re(CO)_2$	a_1	2139.5	2088.7	2092.5	1.0243	1.0225
	b_2	1973.1	1929.5	1924.9	1.0226	1.0250
	a_1	937.3	937.3	886.4	1.0000	1.0574
	b_1	856.7	856.0	813.1	1.0008	1.0536
	b_2	469.9	463.1	458.4	1.0147	1.0251
$OReCO^-$	a′	1827.7	1782.0	1791.4	1.0256	1.0203
	a′	944.3	944.0	894.5	1.0003	1.0557
$ORe(CO)_2^-$	a″	1846.2	1801.6	1806.9	1.0248	1.0217

925.9 and 903.8 cm^{-1}. Both bands showed similar isotopic shifts as their neon counterparts, and split into skewed triplets in the mixed oxygen-16/18 isotopic experiment.

The DFT calculation on this molecule was complicated: eight distinct states (including different spin states and symmetries) were converged within an energy interval of 85 kcal/mol. The lowest doublet state was found as C_{2v} symmetry in a $^2A_2$ electronic state, whereas a $^2B_1$ state is only 1.5 kcal/mol higher, a $^2A_1$ state is 24.9 kcal/mol higher, and the lowest quartet state $^4B_2$ is 37.4 kcal/mol higher. The symmetric and antisymmetric C−O stretching, symmetric and antisymmetric ReO_2 stretching modes, and antisymmetric Re−CO stretching modes were predicted at 2139.5, 1973.1, 937.3, 856.7, and 469.9 cm^{-1}, with intensities of 419, 3511, 61, 204, 84 km/mol, respectively. The BPW91 functional produced comparable frequencies and intensities. The latter three modes agree with the experimental data very well, however, the antisymmetric carbonyl stretching mode is calculated too low and too intense compared to the spectroscopic observation. This problem has been found for the similar $O_2U(CO)_2$ molecule where DFT calculations predicted too much intensity in the antisymmetric C−O stretching mode,[34] and it may arise when two C−O groups are bonded to a heavy metal with a small C−M−C angle.

O_2ReCO. In the argon matrix, the three bands at 2034.1, 982.0, and 929.1 cm^{-1} tracked with each other in all experiments, and are different modes of the same molecule. The 2034.1 cm^{-1} band is appropriate for a carbonyl absorption, and it shifted to 1987.1 and 1989.1 cm^{-1} in the $^{13}CO_2$ and $C^{18}O_2$ experiments, respectively. The band only split into doublets in the mixed $^{12}CO_2/^{13}CO_2$ and $C^{16}O_2/C^{18}O_2$ experiments, which indicates that only one carbonyl ligand is involved. Both 982.0 and 929.1 cm^{-1} bands showed no ^{13}C isotopic displacement but shifted to 928.4 and 883.2 cm^{-1} in the $C^{18}O_2$ experiment. In the mixed oxygen 16/18 experiment, both bands yielded triplet features, with middle components at 965.6 and 896.2 cm^{-1}, respectively. Similar to the ReO_2 stretching modes in the $O_2Re(CO)_2$ molecule, the middle components repelled each other due to the interaction in a lower symmetry $^{16}O-Re-^{18}O$ unit. These three bands at 2034.1, 982.0, and 929.1 cm^{-1} are assigned to the C−O stretching mode, symmetric and antisymmetric ReO_2 stretching modes in an O_2ReCO molecule.

The same three modes were observed for O_2ReCO in the neon matrix. Bands at 2041.1, 988.5, and 938.5 cm^{-1} are assigned to the CO stretching, symmetric and antisymmetric ReO_2 stretching modes. Those bands showed similar behaviors as their argon counterparts in the isotopic substituted samples.

DFT calculation on O_2ReCO was first performed in C_{2v} symmetry, and the lowest state is $^2A_1$. The subsequent vibrational analyses, however, found a small imaginary mode at 38.2 cm^{-1}. Bending CO out of ReO_2 plane only lowered the energy by 0.02 kcal/mol. Most vibrational frequencies for this C_s symmetry $^2A'$ state were very close to values predicted for the C_{2v}, $^2A_1$ state, but importantly no imaginary mode was found (Table 3). The lowest quartet state is 29.7 kcal/mol higher. We believe the $^2A'$ state is the ground state. The predicted CO stretching, symmetric and antisymmetric ReO_2 modes were at 2126.2, 1006.2, and 958.0 cm^{-1}, with relative intensities of 694:34:273. All three modes, and their isotopic ratios agree with the spectroscopic values very well.

$ORe(CO)_2$. Two weak associated bands at 2091.2 and 1976.5 cm^{-1} observed in the argon matrix showed appropriate isotopic shifts for carbonyl stretching vibrations. The 1976.5 cm^{-1} band exhibited triplet features in both mixed $^{12}CO_2/^{13}CO_2$ and $C^{16}O_2/C^{18}O_2$ isotopic experiments; two intermediate components were observed at 1942.4 and 1946.5 cm^{-1}, red-shifted from the medians of pure isotopic absorptions by 11.2 and 18.2 cm^{-1}, respectively. For the 2091.2 cm^{-1} absorption, the splitting patterns in the mixed isotopic experiments were obscured by stronger ^{13}CO and $C^{18}O$ absorptions, only the intermediate bands were observed at 2072.6 and 2073.5 cm^{-1} in the mixed carbon-12/13 and oxygen 16/18 experiments, respectively. These two absorptions at 2091.2 and 1976.5 cm^{-1} are assigned to the symmetric and antisymmetric C−O stretching modes in $ORe(CO)_2$. No Re−O mode was observed for this molecule in the argon matrix.

In the neon matrix, the symmetric and antisymmetric CO stretching modes of the same $ORe(CO)_2$ molecule were observed at 2092.8 and 1984.5 cm^{-1}. Their isotopic shifts and mixed isotopic splitting patterns are listed in the Table 2. Different from the argon matrix, a third tracking mode was observed at 913.6 cm^{-1}. This band did not shift in the $^{13}CO_2$ experiment, and red-shifted to 865.7 cm^{-1} in the $C^{18}O_2$ experiment, with a characteristic oxygen-16/18 isotopic ratio of 1.0553 as a Re−O stretching mode. This band is assigned to the Re−O stretching mode in the $ORe(CO)_2$ molecule.

In the DFT calculation, a C_s symmetry, $^2A'$ ground state was found. The lowest quartet state $^4B_1$ is 14.6 kcal/mol higher, and the lowest C_{2v} symmetry doublet state $^2A_1$ is 14.7 kcal/mol higher in energy. Symmetric and antisymmetric C−O stretching, ReO stretching modes at 2075.1, 1995.4, and 962.6 cm^{-1}, with relative intensities of 546:1860:122 were calculated for the ground state. These results agree well with spectroscopic observations.

$OReCO^-$. A three-band set at 1759.8, 1757.6 and 1754.8 cm^{-1} was observed on deposition in the argon matrix. Different from all aforementioned bands, this band set is photosensitive. It decreased by three-quarters on 15 min $\lambda > 290$ nm irradiation, then was completely destroyed by full-arc mercury lamp irradiation, and did not re-appear on annealing. This band showed red-shifts in both carbon-13 and oxygen-18 isotopic precursor experiments, with average carbon-12/13 and oxygen-16/18 isotopic ratios of 1.0253 and 1.0200, respectively. In both mixed carbon-12/13 and mixed oxygen-16/18 experiments, only doublets were observed, which signifies that only one carbonyl ligand is involved. A very weak band at 923.3 cm^{-1} was found to track with this band set. This weak band did not shift in the $^{13}CO_2$ experiment, and showed characteristic oxygen-18 shift in the $C^{18}O_2$ experiment. No intermediate was observed for this band in the mixed isotopic experiments. The 1757.6 and the 923.3 cm^{-1} bands are assigned to the C−O stretching and Re−O

stretching modes of the $OReCO^-$ anion. Because CCl_4 is well-known for high electron capture cross section, this anion assignment is supported by the spectrum of a CCl_4 doped sample where both bands were essentially eliminated compared to the absorptions of neutral species.[35−37]

In the neon matrix, the same two modes were observed for this $OReCO^-$ anion. New bands at 1771.1 and 930.2 cm^{-1} are assigned to the C−O and Re−O stretching modes, respectively. Both bands were photosensitive, and substantially decreased in the CCl_4-doped sample.

The DFT calculation predicted the ground state of $OReCO^-$ anion as $^1A'$, a planar anion with C_s symmetry, whereas the lowest triplet state $^3A''$ is only 8.6 kcal/mol higher. The vibrational analyses of the $^1A'$ state produced C−O and Re−O stretching modes at 1827.7 and 944.3 cm^{-1}, with relative intensities of 1523:155. The C−O stretching mode has carbon-12/13 and oxygen-16/18 isotopic frequency ratios of 1.0256 and 1.0203, and the Re−O mode has oxygen-16/18 isotopic frequency ratio of 1.0557, which are close to the experimental values. Additional calculation was performed on an isomer, $ReCO_2^-$, and the lowest $^3B_1$ state is 67.6 kcal/mol higher than the $^1A'$ ground-state $OReCO^-$ anion.

$ORe(CO)_2^-$. Another photosensitive band was observed at 1776.6 cm^{-1}. The band only slightly decreased with $\lambda > 290$ nm irradiation, and substantially decreased on full-arc irradiation, but did not regain the absorption intensity in the following annealing experiments. The fact that this band is only affected by a shorter wavelength irradiation signifies that this absorber has higher ionization energy than $OReCO^-$. This band was also eliminated by adding CCl_4 to the CO_2/Ar sample, and hence the band also belongs to an anionic species. It shifted to 1734.7 and 1739.2 cm^{-1} in the $^{13}CO_2$ and $C^{18}O_2$ experiments, with isotopic ratios of 1.0242 and 1.0215. In both mixed $^{12}CO_2/^{13}CO_2$ and mixed $C^{16}O_2/C^{18}O_2$ experiments, this band split into 1:2:1 triplet features with the intermediate components at 1751.7 and 1755.0 cm^{-1}, respectively. Thus, it is clear that two carbonyl ligands are involved in this vibrational mode. In the Re−O stretching region, unfortunately no associated mode was observed. Although it is unlikely that the absorber is $Re(CO)_2^-$ because the neutral product $Re(CO)_2$ was not observed,[37] we cannot determine the number of oxygen atoms attached to the Re atom. Using DFT calculation, which will be discussed later, we tentatively assign this 1776.6 cm^{-1} band to the antisymmetric CO stretching mode of an $ORe(CO)_2^-$ anion.

In the neon matrix, a similar absorption observed at 1787.8 cm^{-1} shifted to 1745.0 and 1750.8 cm^{-1} in the $^{13}CO_2$ and $C^{18}O_2$ experiments. In the mixed $^{12}CO_2/^{13}CO_2$ experiment, a 1:2:1 triplet feature was observed with an intermediate band at 1760.2 cm^{-1}.

The DFT calculation was performed on both $O_2Re(CO)_2^-$ and $ORe(CO)_2^-$ anions. The ground state for $O_2Re(CO)_2^-$ is $^3B_2$ with a C_{2v} symmetry, whereas the lowest singlet state is only 7.0 kcal/mol higher. The $^3B_2$ ground state has the antisymmetric C−O stretching mode at 1896.0 cm^{-1}, and carbon-12/13 and oxygen-16/18 isotopic ratios for this mode were 1.0250 and 1.0214. For the $ORe(CO)_2^-$ anion, the ground state is $^1A'$ with a C_s symmetry. The lowest triplet $^3A'$ state is only 5.1 kcal/mol higher, and the lowest C_{2v} symmetry, singlet $^1A_1$ state is 19.6 kcal/mol higher in energy with an imaginary vibrational mode for bending out of the molecular plane. The antisymmetric C−O mode for the ground $^1A'$ state is calculated at 1846.2 cm^{-1}, and has carbon-12/13 and oxygen-16/18 isotopic ratios of 1.0248 and 1.0217. Compared to the experimental observations at 1776.6 cm^{-1} (argon), 1787.8 cm^{-1} (neon), and their isotopic ratios, we favor the absorber as $ORe(CO)_2^-$.

Reaction Mechanisms. After sample deposition, the strongest product absorption was OReCO, which is formed in exothermic (ΔE results from B3LYP calculations) insertion reaction 1. The lack of OReCO growth on annealing suggests that reaction 1 requires activation energy although secondary reactions with more CO_2 could proceed at about the same rate.

$$Re + CO_2 \rightarrow OReCO \ (\Delta E = -16.5 \text{ kcal/mol}) \quad (1)$$

However, bands for other more complicated products increased slightly on annealing, whereas the OReCO absorptions showed little change, which suggests that the following exothermic processes occur during annealing to form O_2ReCO, $ORe(CO)_2$, and $O_2Re(CO)_2$.

$$OReCO + CO_2 \rightarrow O_2ReCO + CO \ (\Delta E = -14.1 \text{ kcal/mol}) \quad (2)$$

$$OReCO + CO_2 \rightarrow O_2Re(CO)_2 \ (\Delta E = -37.2 \text{ kcal/mol}) \quad (3)$$

$$OReCO + CO \rightarrow ORe(CO)_2 \ (\Delta E = -49.8 \text{ kcal/mol}) \quad (4)$$

The fact that these product absorptions are also observed after sample deposition indicates that reactions (2−4) occur during the deposition process, especially in the neon matrix, since neon solidifies less rapidly at 4 K compared to the more rapid freezing of argon at 7 K.

The anionic species are produced via electron capture during deposition as the laser-ablation process also provides electrons.[10,35−37]

$$OReCO + e^- \rightarrow OReCO^- \ (\Delta E = -55.7 \text{ kcal/mol}) \quad (5)$$

$$ORe(CO)_2 + e^- \rightarrow ORe(CO)_2^- \ (\Delta E = -61.4 \text{ kcal/mol}) \quad (6)$$

Subsequent photoirradiation destroys both anion absorptions through photodetachment processes. The $OReCO^-$ absorptions were removed by $\lambda > 290$ nm radiation, whereas shorter wavelength was needed to eliminate $ORe(CO)_2^-$. This observation is consistent with the higher electronic affinity for $ORe(CO)_2$.

V. Conclusion

Laser-ablated rhenium atoms and electrons react with CO_2 molecules upon co-condensation in excess argon at 7 K and neon at 4 K. Through annealing, photon irradiation, and isotopic substitution, the new OReCO, O_2ReCO, $ORe(CO)_2$, $O_2Re(CO)_2$, $OReCO^-$, and $ORe(CO)_2^-$ species are identified. The anions are not formed in CCl_4 doped samples as ablated electrons are captured instead by the CCl_4 additive. DFT calculations give very good overall agreement between the calculated and observed vibrational frequencies and support the product identification. The OMCO, O_2MCO and $O_2M(CO)_2$ products have also been observed in analogous investigations with Ta and W, and the carbonyl absorptions are generally within 5 to 60 cm^{-1} for these third-row species.[6,10]

Acknowledgment. The authors gratefully acknowledge National Science Foundation support from Grant CHE 00-78836.

References and Notes

(1) Palmer, D. A.; van Eldik, R. *Chem. Rev.* **1983**, *83*, 651.
(2) Culter, A. R.; Hanna, P. K.; Vites, J. C. *Chem. Rev.* **1988**, *88*, 1363.

(3) Gibson, D. H. *Chem. Rev.* **1996**, *96*, 2063.
(4) Gibson, D. H. *Coord. Chem. Rev.* **1999**, *185*−*186*, 335.
(5) Mascetti, J.; Tranquille, M. *J. Phys. Chem.* **1988**, *92*, 2177.
(6) Souter, P. F.; Andrews, L. *Chem. Commun.* **1997**, 777. Souter, P.F.; Andrews, L. *J. Am. Chem. Soc.* **1997**, *119*, 7350.
(7) Zhou, M. F.; Andrews, L. *J. Am. Chem. Soc.* **1998**, *120*, 13 230 (Sc + CO_2).
(8) Zhou, M. F.; Liang, B.; Andrews, L. *J. Phys. Chem. A* **1999**, *103*, 2013 (Cr, Mn, Fe, Co, Ni, Cu + CO_2).
(9) Zhou, M. F.; Andrews, L. *J. Phys. Chem. A* **1999**, *103*, 2066 (V, Ti + CO_2).
(10) Wang, X.; Chen, M.; Zhang, L., Qin, Q. Z. *J. Phys. Chem. A* **2000**, *104*, 758 (Ta + CO_2).
(11) Chen, M.; Wang, X.; Zhang, L. Qin, Q. Z. *J. Phys. Chem. A* **2000**, *104*, 7010 (Nb + CO_2).
(12) Jeung, G. H. *Chem. Phys. Lett.* **1995**, *232*, 319.
(13) Pápai, I.; Mascetti, J.; Fournier, R. *J. Phys. Chem. A* **1997**, *101*, 4465.
(14) Mascetti, J.; Galan, F.; Pápai, I. *Coord. Chem. Rev.* **1999**, *190*−*192*, 557.
(15) Fan, H. J.; Liu, C. W. *Chem. Phys. Lett.* **1999**, *300*, 351.
(16) Sodupe, M.; Branchadell, V.; Rosi, M.; Bauschlicher, C. W., Jr. *J. Phys. Chem. A* **1997**, *101*, 7854.
(17) Scheiring, T.; Klein, A.; Kaim, W. *J. Chem. Soc., Perkin Trans. 2* **1997**, 2569.
(18) Koike, K.; Hori, H.; Ishizuka, M.; Westwell, J. R.; Takeuchi, K.; Ibusuki, T.; Enjouji, K.; Konno, H.; Sakamoto, K.; Ishitani, O. *Organometallics* **1997**, *16*, 5724.
(19) Hori, H.; Koike, K.; Takeuchi, K.; Sasaki, Y. *Chem. Lett.* **2000**, 522.
(20) Sung-Suh, H. M.; Kim, D. S.; Lee, C. W.; Park, S. E. *Appl. Organomet. Chem.* **2000**, *14*, 826.
(21) Burkholder, T. R.; Andrews, L. *J. Chem. Phys.* **1991**, *95*, 8697.
(22) Hassanzadeh, P.; Andrews, L. *J. Phys. Chem.* **1992**, *96*, 9177.
(23) Chertihin, G. V.; Saffel, W.; Yustein, J. T.; Andrews, L. Neurock, M.; Ricca, A.; Bauschlicher, C. W., Jr. *J. Phys. Chem.* **1996**, *100*, 5261.
(24) Zhou, M. F.; Citra, A.; Liang, B.; Andrews, L. *J. Phys. Chem. A* **2000**, *104*, 3457.
(25) *Gaussian 98, Revision A.1.* Frisch, M. J.; Trucks, G. W.; Schlegel, H. B.; Scuseria, G. E.; Robb, M. A.; Cheeseman, J. R.; Zakrzewski, J. A.; Montgomery, J. A.; Stratmann, R. E.; Burant, J. C.; Dapprich, S.; Millam, J. M.; Daniels, A. D.; Kudin, K. N.; Strain, M. C.; Farkas, O.; Tomasi, J.; Barone, V.; Cossi, M.; Cammi, R.; Mennucci, B.; Pomelli, C.; Adamo, C.; Clifford, S.; Ochterski, J.; Petersson, G. A.; Ayala, P. Y.; Cui, Q.; Morokuma, K.; Malick, D. K.; Rabuck, A. D.; Raghavachari, K.; Foresman, J. B.; Cioslowki, J.; Ortiz, J. V.; Stefanov, B. B.; Liu, G.; Liashenko, A.; Piskorz, P.; Komaromi, I.; Gomperts, R.; Martin, R. L.; Fox, D. J.; Keith, T.; Al-Laham, M. A.; Peng, C. Y.; Nanayakkara, A.; Gonzalez, C.; Challacombe, M.; Gill, P. M. W.; Johnson, B. G.; Chen, W.; Wong, M. W.; Andres, J. L.; Head-Gordon, M.; Replogle, E. S.; Pople, J. A. Gaussian, Inc., Pittsburgh, PA, 1998.
(26) Lee, C.; Yang, E.; Parr, R. G. *Phys. Rev. B* **1988**, *37*, 785.
(27) McLean, A. D.; Chandler, G. S. *J. Chem. Phys.* **1980**, *72*, 5639. Wachters, A. J. H. *J. Chem. Phys.* **1970**, *52*, 1033. Hay, P. J. *J. Chem. Phys.* **1977**, *66*, 4377. Raghavachari, K.; Trucks, G. W. *J. Chem. Phys.* **1989**, *91*, 1062.
(28) Hay, P. J.; Wadt, W. R. *J. Chem. Phys.* **1985**, *82*, 270. Wadt, W. R.; Hay, P. J. *J. Chem. Phys.* **1985**, *82*, 284. Hay, P. J.; Wadt, W. R. *J. Chem. Phys.* **1985**, *82*, 299.
(29) Jacox, M. E.; Milligan, D. E. *J. Chem. Phys.* **1971**, *54*, 3935.
(30) Jacox, M. E.; Thompson, W. E. *J. Chem. Phys.* **1989**, *91*, 1410.
(31) Zhou, M. F.; Andrews, L. *J. Chem. Phys.* **1999**, *110*, 2414.
(32) Zhou, M. F.; Andrews, L. *J. Chem. Phys.* **1999**, *110*, 6820.
(33) Bytheway, I.; Wong, M. W. *Chem. Phys. Lett.* **1998**, *282*, 219.
(34) Andrews, L.; Zhou, M. F.; Liang, B.; Li, J.; Bursten, B. E. *J. Am. Chem. Soc.* **2000**, *122*, 11 440.
(35) Zhou, M. F.; Andrews, L. *J. Phys. Chem. A* **1999**, *103*, 7773.
(36) Zhou, M. F.; Andrews, L. *J. Chem. Phys.* **1999**, *110*, 10 370.
(37) Andrews, L.; Zhou, M. F.; Wang, X. Bauschlicher, C. W., Jr. *J. Phys. Chem. A* **2000**, *104*, 8887.